

diffuse scattering is included within the objective aperture. However, the loss of resolution due to chromatic aberration effects is of importance for most present-day high-resolution electron microscopy, so that for quantitative image interpretation, the elastic and inelastic images should be calculated separately with appropriate absorption functions.

It may be noted that, for the conditions of high-resolution imaging which we have discussed, the image intensities are not affected by the correlations of the perturbations of the potential in neighboring atoms. The non-localization of the excitation of the crystal in an inelastic scattering process can influence the elastic scattering only through such correlation effects. The effects of the non-localization can thus appear in the diffraction patterns but do not affect the high-resolution images.

This work was supported by NSF grant DMR 8510059.

References

- AJIKI, N., HASHIMOTO, H., YAMAGUCHI, K. & ENDOH, H. (1985). *Jpn J. Appl. Phys.* **24**, L41-44.
- COENE, W., VAN DYCK, D., VAN TENDELOO, G. & VAN LANDUYT, J. (1985). *Philos. Mag. A*, **52**, 127-143.
- COWLEY, J. M. (1981). *Diffraction Physics*, 2nd ed. Amsterdam: North Holland.
- COWLEY, J. M. & FIELDS, P. M. (1979). *Acta Cryst.* **A35**, 28-37.
- COWLEY, J. M. & MOODIE, A. F. (1957). *Acta Cryst.* **10**, 609-619.
- COWLEY, J. M. & SMITH, D. J. (1987). *Acta Cryst.* **A43**, 737-751.
- DOYLE, P. A. (1969). *Acta Cryst.* **A25**, 569-577.
- DOYLE, P. A. (1970). *Acta Cryst.* **A26**, 133-139.
- DOYLE, P. A. (1971). *Acta Cryst.* **A27**, 109-116.
- KIRKLAND, E. J., LOANE, R. F. & SILCOX, J. (1987). *Ultramicroscopy*, **23**, 77-96.
- KOHL, H. & ROSE, H. (1985). *Adv. Electron. Electron Phys.* **65**, 173-227.
- MARKS, L. D. (1986). *Ultramicroscopy*, **18**, 33-38.
- MISELL, D. L. & ATKINS, A. J. (1973). *J. Phys. A*, **6**, 218-235.
- PIROUZ (1979). *Optik (Stuttgart)*, **54**, 69-74.
- RADI, G. (1970). *Acta Cryst.* **A26**, 41-54.
- STURM, K. (1982). *Adv. Phys.* **31**, 1-64.
- TANAKA, N. & COWLEY, J. M. (1987). *Acta Cryst.* **A43**, 337-346.
- VAN HOVE, L. (1954). *Phys. Rev.* **95**, 249-262.

Acta Cryst. (1988). **A44**, 853-857

Effect of RHEED Resonances on Secondary and Auger Electron Emission of Pt(111) Surfaces

BY H. MARTEN AND G. MEYER-EHMSEN

Fachbereich Physik, Universität Osnabrück, D-4500 Osnabrück, Federal Republic of Germany

(Received 15 December 1987; accepted 25 April 1988)

Abstract

The secondary electron emission, the Auger electron emission and the elastically reflected intensity have been measured simultaneously in a reflection high-energy electron diffraction (RHEED) beam rocking experiment with Pt(111). Secondary and Auger yield depend similarly on incident angle. In particular, both quantities exhibit maxima at primary beam orientations around the resonance maxima of the specular beam intensity. The corresponding primary wave field arising by diffraction in the crystal has been calculated using the dynamical theory of RHEED. It turns out that, in contrast to previous suppositions, at the resonances there is a minimum of primary electron density at the atomic sites. It is shown that the behaviour of both yields is rather a consequence of total primary electron intensity near the surface, which is enhanced at the resonances.

1. Introduction

Owing to inelastic interactions a fast electron beam impinging on a solid can produce different kinds of secondary radiation such as X-rays and Auger elec-

trons (AE) or secondary electrons (SE). These processes are widely used for analysis of small samples, for instance, in the scanning electron microscope.

Owing to diffraction effects of the electron beam in crystals its spatial density distribution is modulated on an atomic scale. The probability of localized inelastic interactions therefore depends on the diffraction conditions fulfilled by the incident beam. On the one hand, this leads to anomalous transmission effects in thin crystals (Honjo & Mihama, 1954; Altenhein & Molière, 1954), which are also well known from X-ray transmission (Borrmann, 1941). On the other hand, an influence of the diffraction condition on the yield of characteristic X-ray emission has been observed for thin metal crystals (Duncumb, 1962; Hall, 1966), as well as for solid samples of ZnS (Miyake, Hayakawa & Miida, 1968). Theoretical interpretations on the basis of the dynamical theory have been given by Hirsch, Howie & Whelan (1962) for the transmission case and by Miyake, Hayakawa & Miida (1968) for the case of reflection. Similarly, the effect of Bragg diffraction of the incident beam on Auger yields of solid samples has been observed (e.g. Morin, 1985).

In the reflection high-energy electron diffraction (RHEED) geometry at small glancing angles a special wave field develops at the so-called 'surface wave resonance' (SWR) condition. Ichimiya & Takeuchi (1983) showed that this gives rise to anomalies in the AE yields of MgO at 10 keV. From the results they concluded that the electron current at the SWR condition is strongly localized at the atomic positions. Actually, the effect was used for a structure determination of Si(111), $\sqrt{3} \times \sqrt{3}$ Ag by a method they called beam rocking Auger electron spectroscopy (BRAES) (Horio & Ichimiya, 1985).

In this paper we present results on SE and AE yields obtained in a recent beam rocking experiment at small glancing angles of incidence with a Pt(111) surface (Marten, 1988) (§ 2) and an interpretation based on the dynamical theory for RHEED (Maksym & Beeby, 1981) (§ 3).

2. Experiment

The experimental RHEED set up has been described in detail by Britze & Meyer-Ehmsen (1978). It has additionally been equipped with a cylindrical mirror analyzer (CMA) (Riber, model OPC 105) in front of the sample and a computer- (Z80-based) controlled beam deflection and data recording system. During the experiments the pressure was about 10^{-8} Pa. The specimen used here was different from that used in earlier experiments with Pt(111) (Marten & Meyer-Ehmsen, 1985). Its surface cleanliness could be controlled more accurately by means of the CMA.

A crystal slice of about 8 mm in diameter and 3 mm in thickness was cut from a single crystalline rod (Goodfellow) by spark erosion, oriented in the [111] direction within 0.1° by Laue diffraction, ground and polished with diamond paste down to $1 \mu\text{m}$ grain. Initial cleaning in an ultra-high-vacuum system was carried out by sputtering (Ne, 500 eV). Special care had to be taken to remove contaminants B, C and P, which was done initially by heating in oxygen, later by flashing up to 1400 K. The surface used in the experiment did not show any contamination in the AE spectrum taken at 3 keV according to the criteria proposed by Mundschau & Vanselow (1985). The RHEED reflections were not streaked but exhibited sharp spots on a Laue circle, which indicates a very flat surface.

The electron energy used was 19 keV. The beam of about $1 \mu\text{A}$ had a diameter of about 1 mm and a divergence of 1 mrad. The SE yield was obtained from the current I_c between crystal and ground potential. Besides the relatively weak diffracted current, I_c contains contributions from the slow so-called true SE ($E \leq 50$ eV) and the fast back-scattered electrons ($E \geq 50$ eV) (Reimer, 1985). By changing the bias voltage applied to the crystal the relative contribution of the SE and back-scattered electrons could be esti-

mated: only about 20% of the outgoing electrons had energies higher than 10 eV. There is an obvious difference between the back-scattering contribution in our experiments and that observed earlier for angles of incidence far from the surface normal (Drescher, Reimer & Seidel, 1970). We suppose this to be an effect of diffraction on back scattering.

While the glancing angle of the incident beam was varied between about 30 and 120 mrad, the energy-filtered intensity of the specular beam, the crystal current and the peak-to-peak amplitude of the Pt NOO Auger line at 64 eV were measured simultaneously. The position of the beam at the surface relative to the CMA entrance had to be adjusted carefully and kept constant to optimize the AE yield. Measurements were carried out for three different planes of incidence, the azimuths being $\langle 2\bar{1}\bar{1} \rangle$, $\langle 2\bar{1}\bar{1} \rangle + 32$ mrad and $\langle 1\bar{1}0 \rangle$.

3. Results and discussion

The experimental results are shown in Figs. 1 to 3 as full curves. It is seen that for each azimuth all measured curves have maxima at approximately the same angles of incidence, as is indicated by the vertical lines. Clearly, these maxima appear to have the same origin. More precisely, however, the maxima of both the SE and AE curves in most cases occur at

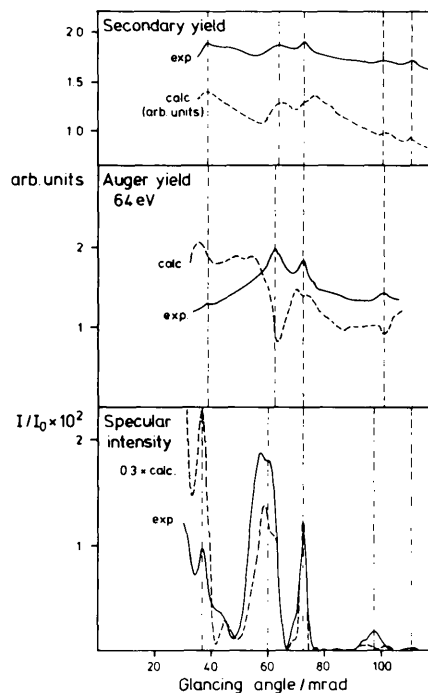


Fig. 1. Pt(111), intensity of the specular beam, Auger yield and secondary electron emission yield vs glancing angle of the incident electron beam at an energy of 19 keV and the azimuth $\langle 1\bar{1}0 \rangle$. — Measurement, - - - calculation including eight atomic layers and seven reciprocal-lattice rods (see text).

somewhat higher angles of incidence than those of the specular beam.

We have shown previously (Marten & Meyer-Ehmsen, 1985) that pairs of prominent maxima in the specular beam intensity for Pt(111) occur at angles just below the threshold angles for the emergence of side beams. These can be ascribed to resonance effects (monolayer resonances), where diffracted beams with small momentum perpendicular to the surface form bound states in the periodic crystal potential normal to the surface. It has also been shown (Meyer-Ehmsen, 1988) that experimental rocking curves of several diffracted beams can be reproduced almost quantitatively by the dynamical theory of Maksym & Beeby (1981), provided that appropriate real and imaginary parts of the crystal potential are used for the calculation.

For an interpretation of our experiments we have calculated rocking curves and the spatial distribution of the primary wave field in the crystal using the theory mentioned. Only a relatively small number of reciprocal-lattice rods in the zeroth Laue zone were taken into account (see figure captions) in order to achieve short computation times (a few seconds per incident angle on an Olivetti M24 personal computer with coprocessor running Turbo Pascal 3.0 code at 8 MHz). Although this will not be exact it is believed to reproduce the main effects of the incident wave field on SE and AE yield. The zeroth-order Fourier

coefficients used are 31 and 6.8 V for the real and the imaginary part of the crystal potential, respectively.

The calculated rocking curves are shown in Figs. 1 to 3. Fig. 4 shows an example of the electron density distribution for the azimuth $\langle 2\bar{1}\bar{1} \rangle$ and a glancing angle corresponding to maximum AE yield, plotted in a similar way to that suggested by Peng & Cowley (1986). It is seen that the electron density decreases rapidly with depth and is indeed strongly modulated. It is also seen that the laterally averaged density is centred around the surface layers as is expected for planar surface channelling under a monolayer resonance situation (Marten & Meyer-Ehmsen, 1985). The density maxima, however, occur off the atomic sites. The same behaviour is found from calculations for a model crystal with half the real and imaginary crystal potentials of Pt. As the density at the atomic sites is very small, atomically localized inelastic interactions are very improbable in this case.

In Figs. 1 to 3 (Auger yield graph) we have plotted as dashed lines the electron density integrated over small disks (0.01 nm in diameter), which would represent the interaction region for a localized excitation process around the centre of the atoms as a function of glancing angle. An escape depth of the AE of four monolayers has been taken into account by an exponentially decreasing weighting factor. Although a few maxima in these curves correspond roughly to observed maxima of the AE yield, mostly broad

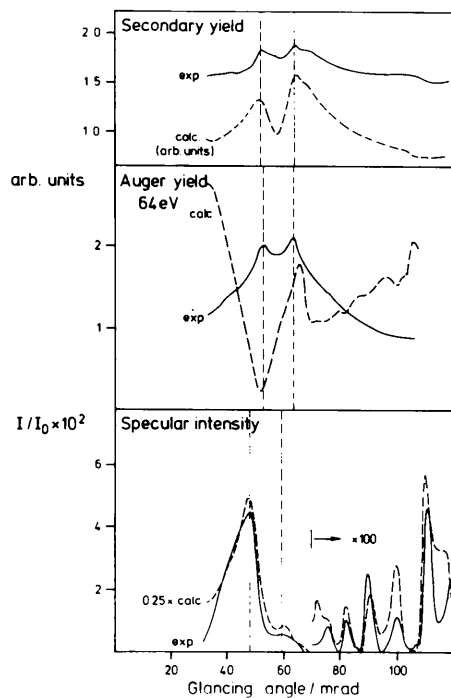


Fig. 2. As Fig. 1. The azimuth is $\langle 2\bar{1}\bar{1} \rangle$. Calculations include five reciprocal-lattice rods.

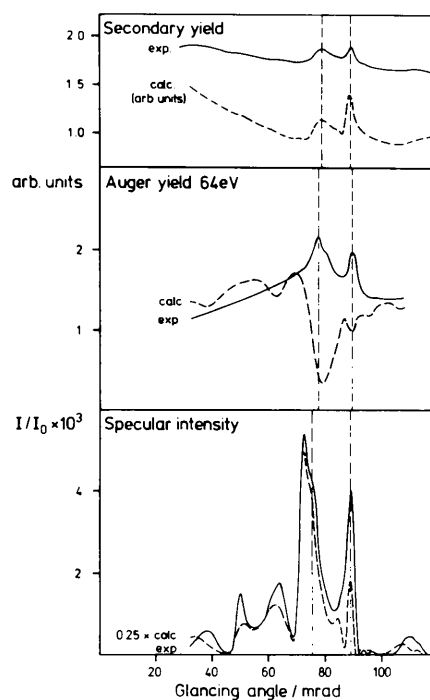


Fig. 3. As Fig. 1. The azimuth is $\langle 2\bar{1}\bar{1} \rangle + 32$ mrad. Calculations include four reciprocal-lattice rods.

minima occur around the angles of observed yield maxima. Clearly, the observed AE emission cannot be explained by the density of the primary electron wave field near the atomic sites. This shows further that localized processes would not necessarily be enhanced at resonance conditions.

In the following we consider the influence of the spatial structure of the wave field on delocalized excitation processes, which govern both the relatively low-energy AE and the SE observed here. The simplest model for this is to assume that the probability of inelastic scattering is constant in space. The number of slow electrons generated will then be proportional to the integral of the primary electron density over the irradiated volume of the crystal. To account for the limited escape probability of the electrons, the integrand is weighted by an exponential containing a mean escape depth L of the electrons, *i.e.* the yield Y is put equal to

$$Y \sim \int |\Phi|^2 \exp(-z/L) dV, \quad (1)$$

where Φ is the wave function of the incident electrons and z is the depth from the crystal surface. It is noted that (1) to some approximation may also describe the contribution due to excitations by inelastically scattered slower electrons, which might be even more effective than the high-energy primaries. This is supposed because the inelastic interactions are mostly also non-localized processes, the probability of which will follow a relation similar to (1).

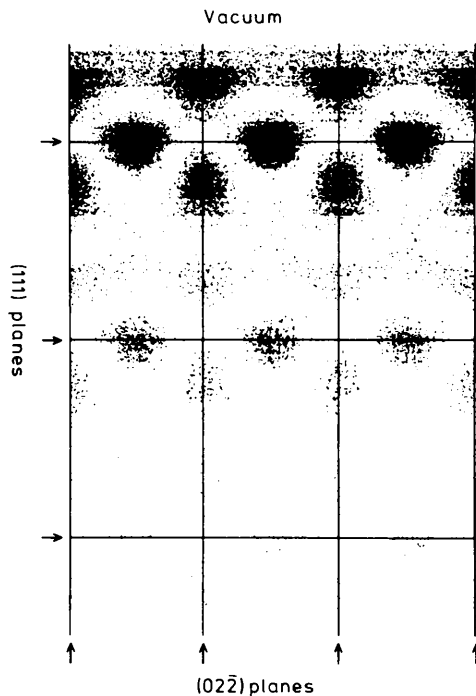


Fig. 4. Spatial density distribution of the incident wave field in a plane perpendicular to the Pt(111) surface, calculated for the azimuth $(2\bar{1}1)$ and a glancing angle of 52.5 mrad.

Results of calculations using (1) with $L=4$ monolayers are given in Figs. 1 to 3 (secondary yield graph) as dashed lines. There is a very satisfying degree of correspondence between the calculated and the measured yield curves, which is rather striking, especially for the SE yield, in view of the simple model used. The general shape of the curves as well as the positions and shapes of the maxima are reproduced very well for all three azimuths. By comparison with the calculated specular beam rocking curves, which are also in good agreement with the measured ones, it is seen further that even the observed angular shift between the maxima in the yields and the rocking maxima is reproduced by the *Ansatz* (1).

We would like to stress that in a RHEED experiment the SE yield can be sampled much more easily than the other quantities dealt with here – simply by measuring the current between crystal and ground – but it contains significant information on the dynamical wave field excited near the surface of the crystal. In this connection it has to be noticed that the angular dependence of (1) is governed by two effects. On the one hand, $|\Phi|^2$ at fixed z varies with angle due to changing amplitudes of the diffracted waves, on the other hand, the penetration of the incident wave into the crystal increases markedly beyond the resonance angles.

In our experiments no influence of Bragg reflections on the yield has been observed, in contrast to the characteristic X-ray emission of ZnS (Miyake, Hayakawa & Miida, 1968) and of thin films (Duncumb, 1962; Hall, 1966). This agrees with the observation that the RHEED reflections from Pt(111) do not show pronounced Bragg maxima but that their main features have to be ascribed to resonance effects (Marten & Meyer-Ehmsen, 1985).

4. Concluding remarks

We have shown experimentally that both the secondary and the Auger electron production by fast electrons (20 keV) from Pt(111) surfaces are markedly enhanced at primary beam orientations around the resonance maxima of the specular beam intensity. By using the dynamical theory of RHEED to calculate the elastic wave field near the surface, we have also shown that at resonance where maxima of the specular beam intensity are observed the primary electron density at the atomic sites may exhibit minima. Localized inelastic interactions of the primary electrons therefore can be very improbable under these conditions. Consequently, the interpretation of angle-dependent yield measurements for localized excitations implies a careful analysis of the primary wave field. On the other hand, for completely delocalized inelastic interaction processes we have found that the observed enhancement of the yields at resonance can be ascribed to the following proper-

ties of the dynamic wave field: (i) at resonance, there is a remarkable increase of the total primary beam current near the crystal surface; (ii) the penetration of the wave field below the corresponding beam emergence threshold is rather small.

References

- ALTENHEIN, H. J. & MOLIÈRE, K. (1954). *Z. Phys.* **139**, 103–114.
 BORRMANN, G. (1941). *Phys. Z.* **42**, 157–170.
 BRITZE, K. & MEYER-EHMSEN, G. (1978). *Surface Sci.* **77**, 131–141.
 DRESCHER, H., REIMER, L. & SEIDEL, H. (1970). *Z. Angew. Phys.* **29**, 331–340.
 DUNCUMB, P. (1962). *Philos. Mag.* **7**, 2101–2105.
 HALL, C. R. (1966). *Proc. R. Soc. (London)*, **295**, 140–163.
 HIRSCH, P. B., HOWIE, A. & WHELAN, M. J. (1962). *Philos. Mag.* **7**, 2095–2100.
 HONJO, G. & MIHAMA, K. (1954). *J. Phys. Soc. Jpn*, **9**, 184–198.
 HORIO, Y. & ICHIMIYA, A. (1985). *Surface Sci.* **164**, 589–601.
 ICHIMIYA, A. & TAKEUCHI, Y. (1983). *Surface Sci.* **128**, 343–349.
 MAKSYM, P. A. & BEEBY, J. L. (1981). *Surface Sci.* **110**, 423–438.
 MARTEN, H. (1988). In *Reflection High-Energy Electron Diffraction and Reflection Electron Imaging of Surfaces*, edited by P. K. LARSEN & P. J. DOBSON, pp. 109–115. New York: Plenum.
 MARTEN, H. & MEYER-EHMSEN, G. (1985). *Surface Sci.* **151**, 570–584.
 MEYER-EHMSEN, G. (1988). In *Reflection High-Energy Electron Diffraction and Reflection Electron Imaging of Surfaces*, edited by P. K. LARSEN & P. J. DOBSON, pp. 99–107. New York: Plenum.
 MIYAKE, S., HAYAKAWA, K. & MIIDA, R. (1968). *Acta Cryst.* **A24**, 182–191.
 MORIN, P. (1985). *Surface Sci.* **164**, 127–138.
 MUNDSCHAU, M. & VANSELOW, R. (1985). *Surface Sci.* **157**, 87–98.
 PENG, L.-M. & COWLEY, J. M. (1986). *Acta Cryst.* **A42**, 545–552.
 REIMER, L. (1985). *Scanning Electron Microscopy*. Berlin: Springer.

Acta Cryst. (1988). **A44**, 857–863

The Octagonal Quasilattice and Electron Diffraction Patterns of the Octagonal Phase

BY Z. M. WANG AND K. H. KUO*

*Laboratory of Atomic Imaging of Solids, Institute of Metal Research, Academia Sinica,
 110015 Shenyang, People's Republic of China*

(Received 5 January 1988; accepted 25 April 1988)

Abstract

An analysis is given of the dual transformation and also the strip method which can yield the ideal octagonal quasilattice as well as its approximants. An ideal octagonal tiling consisting of 45° rhombi and squares can be derived from the projection of a 4D cubic lattice within an irrational 2D subspace onto an irrational 2D hyperplane, and its Fourier transform matches well the eightfold electron diffraction pattern of the Cr–Ni–Si octagonal quasicrystal. The approximant of an octagonal tiling corresponds to the rearrangement of two kinds of tiles in an ideal quasilattice which destroys the exact quasiperiodic sequence. It is shown that the defects introduced to change the aperiodic order into a regular approximant correspond to a linear phason strain along certain directions, and this will break the eightfold rotational symmetry. The Fourier transform agrees well with the experimental electron diffraction pattern displaying only fourfold symmetry.

Introduction

The discovery of a quasicrystal with icosahedral symmetry in an Al–Mn alloy by Shechtman, Blech, Gratias & Cahn (1984) has initiated much activity in the experimental and theoretical studies of non-crystallographic symmetry of aperiodic crystals (Henley, 1987; Kuo, 1988). Quite recently, the discovery of an octagonal quasicrystal in rapidly solidified Cr–Ni–Si and other alloys has been reported by Wang, Chen & Kuo (1987). The diffraction patterns of the new structure show a two-dimensional (2D) quasiperiodicity with eightfold rotational symmetry and one-dimensional periodicity along the eightfold axis. This is rather similar to the 2D decagonal quasicrystal (Bendersky, 1985). The point group symmetry $D_{8h}(8/mmm)$ is incompatible with any periodic lattice and therefore does not occur in crystals. The aperiodic lattice has recently been derived by many methods (Duneau & Katz, 1985; Elser, 1986; Kramer & Neri, 1984; Socolar & Steinhardt, 1986) which are based mainly on de Bruijn's (1981) work on Penrose tilings (Penrose, 1974). In addition, non-crystallographic group theory including the octagonal case

* Also at Beijing Laboratory of Electron Microscopy, Academia Sinica, PO Box 2724, 100080 Beijing, People's Republic of China.